IOP Publishing Journal of Physics A: Mathematical and Theoretical
J. Phys. A: Math. Theor. **52** (2019) 464002 (15pp) https://doi.org/10.1088/1751-8121/ab4a35

Self-consistent Euclidean-random-matrix theory

Walter Schirmacher[1,2,3], Viola Folli[1], Carl Ganter[4] and Giancarlo Ruocco[1,2]

[1] Fondazione Istituto Italiano di Tecnologia (IIT), Center for Life Nano Science, Viale Regina Elena 291, I00161 Roma, Italy
[2] Department of Physics, University of Rome 'La Sapienza', Piazzale Aldo Moro, 5, I00185, Rome, Italy
[3] Institut für Physik, Universität Mainz, Staudinger Weg 9, D-55099 Mainz, Germany
[4] Institut für Radiologie, Technische Universität München, Ismaninger Str. 22, D-81675 München, Germany

E-mail: walter.schirmacher@uni-mainz.de

Received 3 January 2019, revised 25 July 2019
Accepted for publication 2 October 2019
Published 22 October 2019

Abstract

In the present survey we address the vibrational properties of a disordered mass-spring model, in which the spring constants depend exponentially on the distance between the mass positions ('Euclidean-random-matrix model', ERM). Starting from the high-density expansion for this model, introduced by Giorgio Parisi and his coworkers, we present a self-consistent approximation for the vibrational spectrum (SCERM) derived by two of the authors. By a further simplification we arrive at an ERM version of the self-consistent Born approximation (ERM-SCBA). The two approximation schemes describe correctly the transition to a Debye spectrum at low frequencies. In this regime Rayleigh scattering is predicted, which is shown to be a general feature of ERM-type models. Technically Rayleigh scattering involves a non-analyticity of the self energy, which, for the mathematically equivalent transport model, leads to a long-time tail of the velocity autocorrelation function. In the vicinity of an instability the theory predicts both the occurence of a boson peak and anomalous sound attenuation. Finally, we discuss briefly the low-density regime, which is governed by percolation physics.

Keywords: Euclidean random matrices, Rayleigh scattering, boson peak, self-consistent theory

(Some figures may appear in colour only in the online journal)

1. Introduction

Random matrices proved to be good mathematical models for spectra of complex systems [1, 3–8].

A particular class of random matrices occurs in the description of the high-frequency vibrational spectra of amorphous solids and liquids [9–22]. In this context Mézard, Parisi and Zee [23] coined the term *Euclidean random matrix* (ERM) for a geometric model with pairwise connections of randomly distributed points in a d-dimensional euclidean space (see below).

In contrast to the vibrational spectra of crystals, which reflect the crystalline long-range order, the spectra of amorphous materials exhibit several peculiarities or anomalies, which make them very different from their crystalline counterparts [24–28]. These anomalies occur in a frequency range ($\sim$1 THz) much below the Debye frequency, where one expects the density of states (DOS) to obey the Debye law $g(\omega) \propto \omega^2$. One observes instead an enhancement over this law, which, if represented as $g(\omega)/\omega^2$ appears as a maximum. This peak was called 'boson peak', because the temperature dependence of the incoherent scattering intensity could be described by that of the Bose function $n(\omega) + 1 = [1 - \mathrm{e}^{-\hbar\omega/k_\mathrm{B}T}]^{-1}$. Because incoherent neutron and Raman spectra are proportional to this function times the appropriate spectral function [29–31], this means that the spectrum is of harmonic origin. In the same frequency range, below the boson peak, the sound attenuation in many materials increases with the fourth power of the frequency $\Gamma(\omega) \propto \omega^4$ [32, 33], which indicates scattering from frozen-in inhomogeneities (Rayleigh scattering) [20, 34]. Evidence for the boson-peak-related anomalies, including the Rayleigh law, has been obtained as well by molecular-dynamics simulations [35–39] .

These anomalies can be well explained phenomenologically by means of heterogeneous-elasticity theory [28, 38, 40, 41], i.e. by means of the equations of motion of elasticity theory with spatially fluctuating elastic constants, which are solved by field-theoretical techniques [40, 42].

An alternative approach is a microscopic one, i.e. by considering the microscopic equations of motion of a single-component material in the harmonic approximation

$$\frac{\partial^2}{\partial t^2} u_i^\alpha(t) = -\sum_{\beta=1}^{3} \sum_{j=1}^{N_{nn}} t_{ij}^{\alpha\beta} [u_i^\beta(t) - u_j^\beta(t)] \qquad i = 1 \ldots N. \tag{1}$$

Here N is the number of atoms (or 'sites') within the probe volume $V = N/\rho$, where ρ is the site density. $\{u_i^\alpha(t)\}$ are the Cartesian components of the dispacement vector of an atom at location $\mathbf{r}_i$, N_{nn} is the number of nearest neigbours and $t_{ij}^{\alpha\beta}$ are the elements of the force-constant matrix, divided by the atoms' mass m:

$$t_{ij}^{\alpha\beta} = \frac{1}{m} \frac{\partial^2}{\partial x_\alpha \partial x_\beta} \phi(r_{ij}) \tag{2}$$

where $r_{ij} = |\mathbf{r}_i - \mathbf{r}_j|$ is the distance between atoms i and j and $\phi(r)$ is the pairwise interatomic potential in a structurally disordered solid the positions $\mathbf{r}_i$ take random positions, so that $t_{ij}^{\alpha\beta}$ becomes a (sparse) random matrix.

One may now simplify the treatment by ignoring the vector character of the displacements. One then arrives at the following scalar coupled-harmonic oscillator equations (ERM equations) [14–18, 20–22].

$$\frac{\partial^2}{\partial t^2}u_i(t) = -\sum_{j\neq i} t_{ij}[u_i(t) - u_j(t)]. \tag{3}$$

Here the force constants t_{ij} are scalar quantities, which are assumed to be functions of the separation r_{ij}, i.e. $t_{ij} = t(r_{ij})$. If they vanish quickly enough for $r_{ij} \to \infty$ one may perform the j sum in equation (3) over all $N-1$ sites, which are not equal to i. In the present treatment we assume $t(r)$ to be a Gaussian

$$t(r) = \tau_0 \mathrm{e}^{-\frac{1}{2}r^2/\sigma^2}\,, \tag{4}$$

where σ is the interaction range and τ_0 a prefactor.

The scalar ERM model, in fact, has been shown to exhibit both a boson peak [14–17] and Rayleigh scattering [20, 21].

Moreover, there exists an interesting mathematical analogy between the scalar model (3) and a transport equation [12, 43, 44]: if one replaces the double time derivative in equation (3) by a single one, one arrives at an equation of motion, which describes a random walk of a particle on a mesh with nodes at the sites $\mathbf{r}_i$ with transition probabilities t_{ij} and position probabilities u_i. Such a transport occurs with electrons in amorphous solids and in the impurity bands of crystalline semiconductors and is called *hopping transport* [2, 45, 46]. In the steady state ($\frac{\partial u_i}{\partial t} = 0$) one further obtains a mathematical equivalence to a set of Kirchhoff's equations of an electrical network with conductances t_{ij} and nodal voltages u_i [2, 46, 47].

The purpose of the present work is (i) to give a survey over the results obtained so far for the ERM model, and (ii) establish a relationship between the self-consistent approximation of the ERM model and the self-consistent Born approximation (SCBA) of heterogeneous-elasticity theory.

In the next section we introduce the ERM formalism and summarize the lowest-order results for the high-density expansion. In the third section we motivate the self-consistent ERM approximation (SCERM appr.). We show that a simplified version of it (ERM-SCBA) becomes mathematically equivalent to the SCBA. In the fourth section we discuss the hydrodynamic regime (small frequencies and wavenumbers) and show, using a coarse-graining procedure that in this regime one has always Debye wave behavior and Rayleigh scattering. We end with a discussion of the low-density regime and with conclusions.

2. ERM theory

2.1. Formalism

In frequency space the dynamics of the ERM model is described by

$$su_i(s) = -\sum_{j\neq i} t_{ij}\big[u_i(s) - u_j(s)\big] = -\sum_j D_{ij}u_j(s). \tag{5}$$

Here D_{ij} is the dynamical matrix defined by

$$D_{ij} = \begin{cases} \sum_\ell t_{i\ell} & i = j \\ -t_{ij} & i \neq j \end{cases} \tag{6}$$

$$\sum_j D_{ij} = 0\,. \tag{7}$$

For the vibrational problem the sum rule (7) is due to momentum conservation ($\leftrightarrow$ translational invariance), for the transport problem (7) represents particle number conservation, and for the network (7) is due to current conservation.

For vibrational spectra the complex inhomogeneity takes the form $s = -\omega^2 - \mathrm{i}\epsilon = -\lambda - \mathrm{i}\epsilon$, and $u_i(s)$ represents the vibrational elongation. Here $\omega^2 = \lambda$ is the eigenvalue of the dynamical matrix D, and ω the frequency corresponding to the time derivative. For the description of hopping transport and diffusion $s = -\mathrm{i}\omega + \epsilon$, and $u_i(s)$ represents the position of a random walker.

An important parameter of the ERM model is the density of points $\rho = N/V$ and its relation to the interaction range σ, quantified by $\Gamma^{-1} = \rho\sigma^3$. In the high-density limit Γ serves as a small parameter for perturbation theory [15, 18, 20, 23]. In the opposite limit $\Gamma \to \infty$ the model is dominated by percolation physics [2, 46, 48–51], because—in the transport problem—the current goes along the path of least resistance.

The quantity of interest is the $\mathbf{q}$ dependent averaged Green's function

$$\begin{aligned} G(\mathbf{q},s) &= \left\langle \frac{1}{N}\sum_{\ell m} \mathrm{e}^{\mathrm{i}\mathbf{q}(\mathbf{r}_\ell - \mathbf{r}_m)} [s+\mathbf{D}]^{-1}_{\ell m} \right\rangle \\ &= \frac{1}{s} + \sum_{p=1}^{\infty} (-1)^p \frac{1}{s^{p+1}} \frac{1}{N} \sum_{i_0 \ldots i_p} \left\langle \mathrm{e}^{\mathrm{i}\mathbf{q}\mathbf{r}_{i_0 i_1}} D_{i_0 i_1} \ldots \mathrm{e}^{\mathrm{i}\mathbf{q}\mathbf{r}_{i_{p-1} i_p}} D_{i_{sp-1} i_p} \right\rangle \\ &= \frac{1}{s + t_0 - t(q) - \Sigma(\mathbf{q},s)}. \end{aligned} \tag{8}$$

The angle brackets denote a configuration average. The particle positions $\mathbf{r}_\ell$ are assumed to be independently distributed, i.e. the joint probability density factorizes

$$P(\mathbf{r}_1, \mathbf{r}_2, \ldots \mathbf{r}_N) = p(\mathbf{r}_1)\, p(\mathbf{r}_2) \cdot \cdots \cdot p(\mathbf{r}_N) \tag{9}$$

with

$$p(\mathbf{r}_\ell) = \frac{1}{V}. \tag{10}$$

The second line of equation (8) is a high-frequency expansion, which is, due to the increasing number of internal summation over the particle positions also a high-density expansion with respect to the parameter $\Gamma = [\rho\sigma^3]^{-1}$. In the third line the Green's function is represented in terms of the Fourier-transformed force constants

$$t(q) = \rho \int_V \mathrm{d}^3\mathbf{r}\, t(r) \mathrm{e}^{\mathrm{i}\mathbf{q}\mathbf{r}} = t_0 \mathrm{e}^{-\frac{1}{2}\mathbf{q}^2\sigma^2}, \tag{11}$$

with $t_0 = \rho \int_V \mathrm{d}^3\mathbf{r}\, t(r) = \tau_0 \frac{(2\pi)^{3/2}}{\Gamma}$, and the self-energy function $\Sigma(\mathbf{q},s)$. The level density is obtained from the Green's function via

$$\rho(\lambda) = \frac{1}{\pi} \mathcal{I}m\{G_\infty(s)\} \tag{12}$$

with $G_\infty(s) = \lim_{|\mathbf{q}|\to\infty} G(\mathbf{q},s)$. The usual DOS is obtained from the level density as

$$g(\omega) = \left|\partial\lambda/\partial\omega\right| \rho(\lambda) = 2\omega\rho(\lambda). \tag{13}$$

In particular, the Debye DOS $g(\omega) \propto \omega^2$ for plane waves corresponts to $\rho(\lambda) \propto \lambda^{1/2}$.

The self energy can be (and has been [15, 16, 20]) calculated with increasing powers of the inverse density ρ.

The lowest-order result is $\Sigma^{(0)}(\mathbf{q}, s) = 0$, so that in the high-density limit

$$G^{(0)}(\mathbf{q}, s) = \frac{1}{s + t_0 - t(q)}. \tag{14}$$

The function $t_0 - t(q) \equiv \omega^2(q)$ may be interpreted as the square of a high-frequency 'liquid dispersion' [9], which starts at small q quadratically (acoustic dispersion limit) and saturates at t_0, which might be interpreted as the square of an Einstein frequency [9].

As shown in [20, 21] and in section 3, for small q the self-energy $\Sigma(q, s)$ varies as well with q^2 and exhibits a non-analyticity

$$\Sigma(q, s) \propto q^2 s^{3/2}. \tag{15}$$

The disorder-induced imaginary part of Σ gives rise to a finite width $\delta\omega$ of the line, characterized by the dispersion $\omega(q)$, which, in the limit $q \to 0$ is given by

$$\delta\omega \propto \omega \mathcal{I}\mathrm{m}\{\Sigma(q, s)\} \propto q^2 \Gamma(\omega)\,, \tag{16}$$

where $\Gamma(\omega)$ is the sound attenuation coefficient, the latter varies as $\Gamma \propto \omega^4$ (Rayleigh scattering). In all approximate calculations of $\Sigma(q, s)$ one must make sure that the property (15) is retained.

The lowest-order nontrivial contribution to the self energy is [15, 16, 20]

$$\Sigma^{(1)}(\mathbf{q}, s) = \sum_{\mathbf{p}} \Big[t(\mathbf{p} - \mathbf{q}) - t(\mathbf{p})\Big]^2 G^{(0)}(\mathbf{p}, s). \tag{17}$$

Here $\sum_{\mathbf{p}}$ denotes $\frac{1}{\rho(2\pi)^3} \int \mathrm{d}^3\mathbf{p}$.

The second-order contribution to $\Sigma(q, s)$ has been explicitly shown [20, 52] to exhibit the non-analyticity (15), contrary to claims in [15, 16]. In particular it was shown that this contribution may be grouped into different classes with respect to the appearance of the diagonal or off-diagonal elements of the dynamical matrix (6), and that the sum of the self-energy contributions of each class exhibit Rayleigh scattering (15) individually.

3. Self-consistent ERM approximations

3.1. SCERM approximation

It has been suggested [15, 16] that one might obtain a suitable self-consistent (i.e. non-perturbative) approximation by replacing $G_0(\mathbf{p}, s)$ in (17) by the full Green's function $G(\mathbf{p}, s)$ ('cactus approximation'). However, as shown by [20], this self-consistent scheme violates the Rayleigh-scattering requirement (15). This is so, as shown in [20], because if one makes a high-density expansion of the cactus self energy, the second-order term does not coincide with one or the sum of several class sums of the exact second-order contributions.

A self-consistent scheme for calculating the self-energy, which preserves this property has been proposed [20] by making sure that, if the self-consistent self-energy is expanded in terms of the inverse density only entire sums of the different classes of self-energy diagrams are retained. This was achieved by introducing auxiliary quantities $g(\mathbf{q}, s)$ and $\sigma(\mathbf{q}, s)$.

Within this self-consistent ERM (SCERM) approximation the self energy is given by[5]

$$\Sigma(\mathbf{q},s) = \sum_{\mathbf{p}} \Big[t(\mathbf{q}-\mathbf{p}) - t(p)\Big]^2 g(p,s). \tag{18}$$

The auxiliary quantities $\sigma(\mathbf{q},s)$ and $g(\mathbf{q},s)$ obey the self-consistent set of equations

$$g(q,s) = \Big[s + t_0 - t(q) - \sigma(q,s)\Big]^{-1} \tag{19}$$

$$\sigma(\mathbf{q},s) = \sum_{\mathbf{p}} \Big[t(\mathbf{q}-\mathbf{p}) - t(p)\Big]\Big[t(\mathbf{q}-\mathbf{p}) - t(q)\Big] g(p,s). \tag{20}$$

For calculating the level density we need the large-wavenumber limit of the Green's function and the self energy $\Sigma_\infty(s)$, equation (24).

In the $|\mathbf{q}| \to \infty$ limit the Green's function of equation (8) becomes (taking into account $\lim_{|\mathbf{q}|\to\infty} t(q) \to 0$

$$G_\infty(s) = \Big[s + t_0 - \Sigma_\infty(s)\Big]^{-1}. \tag{21}$$

In order to perform the $|\mathbf{q}| \to \infty$ limit for the self energy correctly, it is advisable to reformulate equation (18), using the identy,

$$\sum_{\mathbf{p}} h_1(\mathbf{q}-\mathbf{p}) h_2(\mathbf{p}) = \sum_{\mathbf{p}} h_2(\mathbf{q}-\mathbf{p}) h_1(\mathbf{p}) \tag{22}$$

as

$$\Sigma(\mathbf{q},s) = \sum_{\mathbf{p}} \Big[t(p) - t(\mathbf{q}-\mathbf{p})\Big] t(p) \Big[g(p,s) + g(\mathbf{q}-\mathbf{p},s)\Big]. \tag{23}$$

The $|\mathbf{q}| \to \infty$ limit is then

$$\Sigma_\infty(s) = \sum_{\mathbf{p}} t^2(p) \Big[g(p,s) + g_\infty(s)\Big]. \tag{24}$$

These expressions contain the large-wavenumber limit of the auxiliary quantities $\sigma_\infty = \lim_{q\to\infty} \sigma(q,s)$ and $g_\infty = \lim_{q\to\infty} g(q,s)$. In order to calculate these quantities we take the large wavenumber limit in the self-consistent equations (19) and (20).

Applying again the convolution identity (22) to obtain

$$\sigma_\infty = \sum_p t(p)^2 \, g_\infty \tag{25}$$

$$g_\infty = \frac{1}{s + t_0 - \sigma_\infty} = \frac{1}{s + t_0 - \sum_p t(p)^2 g_\infty} \tag{26}$$

(25) and (26) lead to a quadratic equation for g_∞ with the solution ('Hubbard Green's function' [53])

[5] This relation between $\Sigma(\mathbf{q},s)$ and the auxiliary quantities $g(\mathbf{q},s)$ and $\sigma(\mathbf{q},s)$ has been called [20] 'cactus-1 approximation'. A more complicated relation ('cactus-2 approximation'), which contains one more class sum in the second-order expansion, [20] shall not be considered here.

$$g_\infty(s) \doteq g_{\rm HE}(s) = \frac{2}{s+t_0+\sqrt{[s+t_0]^2-4\sum_p t(p)^2}}. \tag{27}$$

Its imaginary part is a half-ellipse (HE), centered around t_0 with half width $2\sqrt{\sum_p t^2(p)}$

Combining now (24) and (25) we have

$$\Sigma_\infty(s) = \Sigma_\infty^{(1)}(s) + \sigma_\infty(s) \tag{28}$$

with

$$\Sigma_\infty^{(1)}(s) = \sum_p t(p)^2 g(p,s). \tag{29}$$

Combining this with the expression (21) for $G_\infty(s)$ we get

$$G_\infty(s) = g_\infty\big(s-\Sigma_\infty^{(1)}(s)\big) = g_{\rm HE}\big(s-\Sigma_\infty^{(1)}(s)\big). \tag{30}$$

For the level density we then obtain

$$\rho(\lambda) = \frac{1}{\pi}\mathcal{I}m\Big\{g_{\rm HE}\big(s-\Sigma_\infty^{(1)}(s)\big)\Big\} \tag{31}$$

with $g_{\rm HE}(s)$ given by (27) and $\Sigma_\infty^{(1)}(s)$ according to (29).

The self-consistent equations (18)–(20) together with (29) and (31) establish the SCERM scheme for calculating the level density.

3.2. ERM self-consistent Born approximation (ERM-SCBA)

We now further simplify the SCERM equations as follows [22]:

If we consider the self-consistency equations (19) and (20) we realize that the main contributions to the integrals over wavevectors are restricted to $|\mathbf{q}| < 1/\sigma$. This means that we do not make a big error, if we perform an expansion with respect to the parameter $|\mathbf{q}|\sigma$, i.e. a *hydrodynamic* expansion. For $t(q)$ we can write

$$t(q) = t_0 - q^2 c_0^2 \tag{32}$$

where

$$c_0^2 = -\frac{1}{2}\frac{\partial^2}{\partial q^2}t(q)\bigg|_{q=0} = \frac{1}{2}t_0\sigma^2 \tag{33}$$

is the unrenormalized sound velocity. We now define a hydrodynamic self energy

$$\sigma_1(s) = \lim_{q\to 0}\frac{1}{q^2}\sigma(q,s) \tag{34}$$

so that the hydrodynamic version of the auxiliary Green's function becomes

$$g(q,s) = \frac{1}{s+q^2(c_0^2-\sigma_1(s))}. \tag{35}$$

By performing a small-p expansion of the vertices in equations (18) and (20) we obtain the following equation for $\sigma_1(s)$ [22]:

$$\sigma_1(s) = \frac{7}{6} c_0^2 \sum_p p^2 \big[-t'(p)/p \big] g(p,s). \tag{36}$$

Introducing the dimensionless wavenumber $\tilde{p} = \sigma p$ and the dimensionles self energy $\tilde{\sigma}_1(s) = \sigma_1(s)/c_0^2$ we obtain

$$\tilde{\sigma}_1(s) = \gamma \frac{1}{I_0} \int_0^\infty \mathrm{d}\tilde{p} \tilde{p}^4 \big[-t'(\tilde{p})/\tilde{p} \big] \frac{1}{s\sigma^2/c_0^2 + \tilde{p}^2 \big[1 - \tilde{\sigma}_1(s) \big]} \tag{37}$$

with the normalization constant

$$I_0 = \int_0^\infty \mathrm{d}\tilde{p} \tilde{p}^2 \big[-t'(\tilde{p})/\tilde{p} \big] = \frac{\sqrt{\pi}}{2} \tag{38}$$

and the 'disorder parameter'

$$\gamma = \frac{7}{6\pi^2} I_0 \frac{t_0 \sigma^2}{c_0^2} \Gamma = \frac{7}{6} \frac{1}{\pi^{3/2}} \Gamma. \tag{39}$$

The self-consistent equations (35), (36) and (or, equivalently equation (37)) together with (29) and (31) establish the ERM-SCBA.

We call this version SCBA, because the ERM-SCBA equations are almost the same as those derived from a model of elastic waves with fluctuating local elastic coefficients (heterogeneous-elasticity theory, [40, 41]).

In the SCBA of heterogeneous-elasticity theory the disorder parameter γ is the relative variance of the elastic-constant fluctuations $\Delta G(\mathbf{r}) = G(\mathbf{r}) - \langle G \rangle$

$$\gamma = V_c \frac{\langle \Delta G^2 \rangle}{\langle G \rangle^2}. \tag{40}$$

Here V_c is the coarse-graining volume used to calculate the fluctuating elastic coefficients from a more microscopic description [38]. The relative variance of the force constants $t(\mathbf{r})$ can be calculated exactly [22] with the result

$$\frac{\langle \Delta t^2 \rangle}{\langle t \rangle^2} = \frac{1}{\langle t \rangle^2} \big[\langle t^2 \rangle - \langle t \rangle^2 \big] = \frac{1}{2\pi^{3/2}} \Gamma. \tag{41}$$

So the density parameter Γ can be identified with the disorder parameter γ of heterogeneous-elasticity theory. The lower the density in the ERM model the stronger is the disorder.

3.3. General features of the ERM model at high densities

In figure 1 we compare the level density obtained by a numerical simulation of the ERM vibrational model with Gaussian force constants [22] with the results of SCERM and ERM-SCBA. In figure 2 we compare the spectrum calculated in ERM-SCBA with the numerically calculated one for several densities. The spectrum at high densities (Γ comparable to or smaller than 1) is dominated by an Einstein-like peak situated at $\lambda = t_0$, which is given by an average over all force constants (proportional to the first spectral moment [22]). Its width is essentially given by the variance of the force constants (proportional to the second spectral moment [22]). A completely incoherent average over the local vibrations à la Einstein, however, would give an exponentially decreasing level density at small eigenvalues. Instead, we have a cross-over to a Debye $\lambda^{1/2}$ law as evidenced in the inset of figure 2. This means that the mass-spring model, represented by the vibrational version of the ERM model, allows for the propagation of

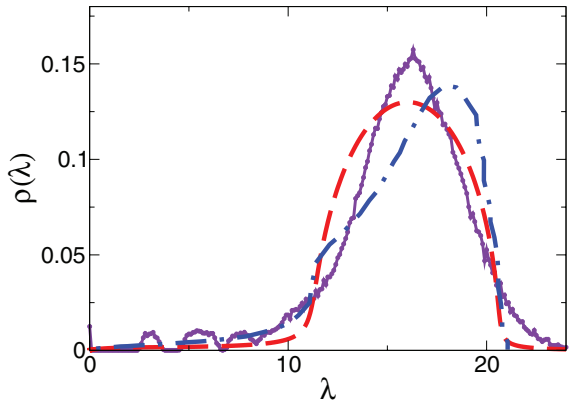

Figure 1. Comparison between the numerically calculated level density ($N = 800$) for $\Gamma = 1$ (violet connected symbols) with the result of the self-consistent ERM approximation (SCERM), equations (18)–(20), (29) and (31), [20] (blue dash-dots), and that of the ERM-SCBA (29), (31), (35) and (36), (red dashes).

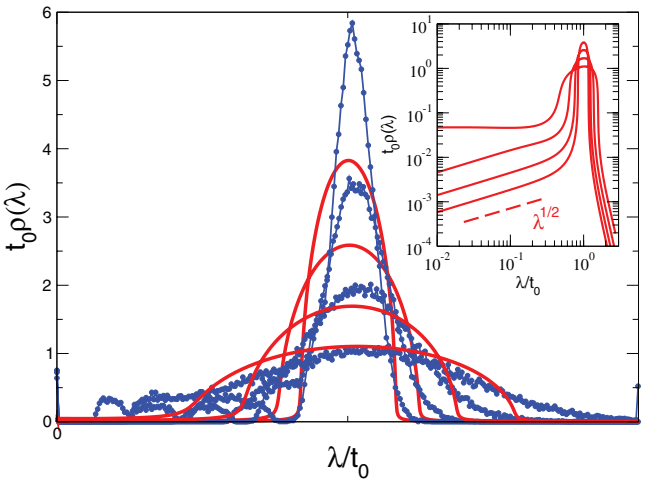

Figure 2. Comparison between the numerically calculated level density ($N = 200$, connected symbols) with the results of ERM-SCBA (red lines) for $\Gamma = 0.3$ (red dashes), 0.65 (orange dash-dots), 1.5 (green dash-doubledots) and 3.5 (blue full lines). Inset: ERM-SCBA data in double-logarithmic representation. The dotted line indicates a $\lambda^{1/2}$ dependence.

waves: in the frequency regime, where the level density shows the $\lambda^{1/2}$ behaviour, the eigenfunctions of the dynamical matrix are approximately plane waves. As the system is certainly disordered, therefore, one expects that the scattering of these waves obeys Rayleigh's ω^4 law.

By a diagrammatic analysis it was shown in [20] to second order in the inverse density that the ERM model, in fact, has this feature, which corresponds to a non-analytic dependence of the self energy's imaginary part as $\Sigma''(\lambda) \propto \lambda^{3/2}$. By a coarse-graining procedure they showed that the Rayleigh scattering is a general propertiy of models of the type (5) with sufficient short-range correlations/interactions (see next section). Later, by a field-theoretic procedure Grigera *et al* [21] showed to all orders that the ERM model has this property.

3.4. Instability and the boson peak

It is well known that the eigenvalues of a dynamical matrix of the form (6) with non-negative entries t_{ij} are all non-negative, which may be easily proved using Gershgorin's theorem [55].

However, if we reduce the density below $1/\Gamma^* \approx 1/2.37$ the ERM-SCBA predicts a transition towards an unstable spectrum with values of λ smaller than 0. While this is obviously an artefact of the SCBA approximation, such an instability can happen for models in which some of the force constants take negative values [13, 17–19, 40, 56]. The instability of the SCBA may be rationalized as follows: using a model with fluctuating elastic constants the SCBA may be derived within a replica-field theoretical framework by a saddle-point approximation, in which the inverse of the disorder parameter γ serves as a large parameter. Within this derivation it is assumed that the fluctuations have a Gaussian distribution with width γ. From this assumption it is clear that beyond a critical γ^* an instability occurs, because too many negative elastic constants are present. In a vector description it is the shear elasticity, which—via very small and negative local values—causes the instability [38, 40, 56].

Within the ERM model the instability can be made real by explicitly introducing partly negative force constants t_{ij} [13, 17]. As a precursor of the instability a deviation of the level density from the Debye $g(\lambda) \propto \lambda^{1/2}$ (or $g(\omega) \propto \omega^2$) law is obtained, as depicted in figure 3. Such a deviation, called 'boson peak', has been observed experimentally in glasses and other disordered materials and has been subject to an intense dispute[6].

It is clear that near a harmonic instability the anharmonic interaction becomes important, which has been shown by Tomaras *et al* [57] to contribute a term $\Gamma(\omega) \propto \omega^2$ to the sound attenuation. If the anharmonic term is included, the combined anharmonic and unstable configuration produce a critical spectrum $g(\omega) \propto \omega^{3/2}$ as well as a critical attenuation $\Gamma(\omega) \propto \omega^{3/2}$ [18, 56, 58]. Such a behavior of the sound attenuation has, indeed, been observed in the GHz range in a network glass [59].

4. Coarse-graining, Rayleigh scattering and long-time tail of the transport velocity correlations

We consider the network transport problem defined in (5). We tile the total volume V into boxes of volume $V_c \ll V$. For a given box with volume V_c the conductance of the network inside the box and hence the conductivity and diffusivity can be calculated [2, 46]. We call this diffusivity $D_{V_c}(\mathbf{r}) = D_0 + \delta D_{V_c}(\mathbf{r})$, where $\mathbf{r}$ is the vector pointing to the center of the box and $D_0 = \langle D_{V_c}(\mathbf{r})\rangle$ (disorder average).

In the coarse-grained system we deal with a *spatially fluctuating diffusivity* obeying the following equation of motion for the continuous density $n(\mathbf{r}, s)$

$$sn(\mathbf{r}, s) = \nabla D_{V_c}(\mathbf{r}) \nabla n(\mathbf{r}, s). \tag{42}$$

As before for the transport problem $s = -\mathrm{i}\omega + \epsilon$. For the mathematically equivalent vibrational problem ($s = -\omega^2 - \mathrm{i}\epsilon$) D_{V_c} takes the role of a spatially fluctuating elastic modulus, or squared sound velocity v^2. $n(\mathbf{r}, s)$ plays the role of the scalar vibrational amplitude $u(\mathbf{r}, s)$.

[6] See [28] for many references dealing with the boson peak.

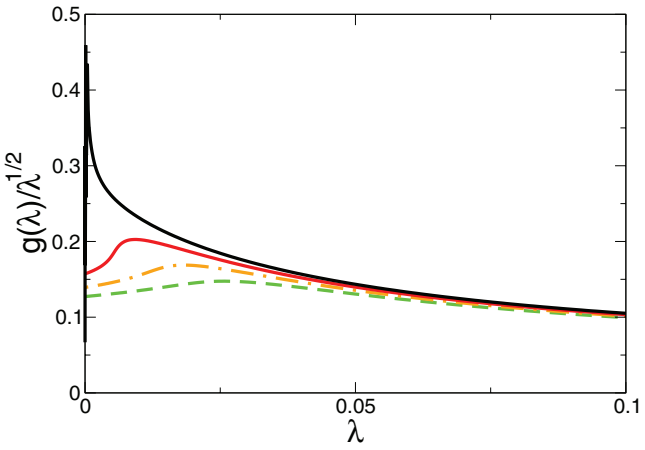

Figure 3. Reduced DOS $g(\lambda)/\sqrt{\lambda}$ for the inverse densities (from bottom to top) $\Gamma = 2.28, 2.32, 2.36, 2.40$.

The Green's function corresponding to equation (42) obeys the equation of motion

$$\big(s - \nabla\big[D_0 + \delta D_{V_c}(\mathbf{r})\big]\nabla\big)G(\mathbf{r},\mathbf{r}',s) = \delta(\mathbf{r}-\mathbf{r}')\,, \tag{43}$$

from which a recursion formula for the Green's function in $\mathbf{q}$ space

$$G(\mathbf{q},\mathbf{q}',s) = \frac{1}{V}\int \mathrm{d}\mathbf{r}\int \mathrm{d}\mathbf{r}' \mathrm{e}^{-\mathrm{i}\mathbf{q}\mathbf{r}}\mathrm{e}^{\mathrm{i}\mathbf{q}'\mathbf{r}'}G(\mathbf{r},\mathbf{r}',s) \tag{44}$$

in terms of the unperturbed Green's function $G_0(q,s) = [s + D_0 q^2]^{-1}$ can be derived [60]. Averaging over (44) one arrives at a representation

$$\langle G(\mathbf{q},\mathbf{q}',s)\rangle = \delta_{\mathbf{q},\mathbf{q}'}\frac{1}{G_0^{-1}(q,s) - \Sigma(\mathbf{q},s)} \tag{45}$$

in terms at a self-energy function, which is obtained to second order in the fluctuations δD_{V_c} as

$$\Sigma(\mathbf{q},s) = \frac{1}{(2\pi)^d}\int \mathrm{d}^d\mathbf{p} K_{V_c}(\mathbf{q}-\mathbf{p})(\mathbf{q}\cdot\mathbf{p})^2 G_0(\mathbf{p},s) \tag{46}$$

where

$$K_{V_c}(\mathbf{q}) = \int \mathrm{d}^d\mathbf{r}\mathrm{e}^{\mathrm{i}\mathbf{q}\mathbf{r}}\langle \delta D_{V_c}(\mathbf{r}_0+\mathbf{r})\delta D_{V_c}(\mathbf{r}_0)\rangle \tag{47}$$

is the Fourier-transformed correlation function of the diffusivity fluctuations, and $d \geqslant 2$ is the dimensionality. For $t(r)$ falling off rapidly enough with distance r $K_{V_c}(0)$ is finite, and we can write

$$K_{V_c}(\mathbf{q}) = \sigma' f_{V_c}(q) \tag{48}$$

with $f_{V_c}(q) = 1$ for $q < q_c = 2\pi/V_c^{1/d}$ and 0 elsewhere. σ' is the variance of the diffusivity (squared sound velocity) per volume. Relation (46) is the *Born approximation* for the coarse-grained problem.

In the long-wavelength limit $q \to 0$ we obtain

$$\Sigma(\mathbf{q}, s) \propto q^2\sigma' \int_0^{k_c} \mathrm{d}p \frac{p^{d+1}}{s + D_0 p^2} \,. \tag{49}$$

If we define

$$D(s) = D_0 - \lim_{q\to 0} \frac{1}{q^2}\Sigma(q, s) \equiv D_0 + \Delta D(s) \tag{50}$$

we obtain for $|s| \to 0$ from equation (49) a contribution to $D(s)$, which is non-analytic in the complex variable s, namely

$$\Delta D(s) \propto s^{d/2} \qquad \text{for } s \to 0. \tag{51}$$

For the transport problem it can be shown that the frequency-dependent diffusivity is the Laplace transform of the velocity autocorrelation function $Z(t)$ [61]. Therefore (51) implies

$$Z(t) \propto t^{-(d+2)/2} \quad \text{for} \quad t \to \infty \tag{52}$$

which is a longtime tail typical for single-particle transport in a quenched-disordered environment [60, 62, 63].

On the other hand, for the vibrational problem this non-analyticity leads to *Rayleigh scattering* for the sound-attenuation coefficient

$$\Gamma(\omega) \propto \omega \lim_{q\to 0} \frac{1}{q^2}\mathcal{I}\mathrm{m}\{\Sigma(q, s)\} \propto \omega^{d+1}. \tag{53}$$

This means that Rayleigh scattering is a general feature of ERM-type models or other models with a disordered local elasticity coefficient of type (42). It is remarkable that Rayleigh scattering and the long-time tail have the same mathematical origin, namely the integral (35) over the diffusion propagator (free wave propagator). For long-range fluctuations, for which $K_{V_c}(q)$ diverges in the long-wavelength limit, the Rayleigh law is modified, as has been pointed out recently [64].

5. Remarks on the low-density regime

As indicated in the introduction, the low-density regime $\Gamma \ll 1$ of the ERM-type models is governed by percolation physics [2, 46, 48–51]. For models, in which the force constants t_{ij} vary exponentially with the site separation r_{ij}, in the low-density regime the variations of the t_{ij} cover many orders of magnitude. In an electrical network of conductances $t_{ij} = t(r_{ij})$ a connection via a small separation therefore essentially is a short circuit, compared to longer separations. Therefore one has devised a 'percolation construction' [2, 43, 46] for the calculation of the conductance of a low-density network, which proceeds as follows: all conductances $t(r_{ij})$ are sorted by their magnitude (or separation). The largest conductances, i.e. larger than a certain threshold $t_{\mathrm{thr}} = t(r_{\mathrm{thr}})$ (corresponding to those with small site separations $r_{ij} \leqslant r_{\mathrm{thr}}$) are tinned into the network first. Then the threshold is decreased until at $t^* = t(r^*)$ a path through the sample is established, the percolation path. The conductance is then just t^*, because all other conductances act as shorts in comparison to t^*. In comparison with all other paths, which

lead through the sample, the percolation path has the largest conductance, i.e. the smallest resistance. Therefore the percolation path is the path of smallest resistance through the system. The percolation construction is identical to the percolation problem of overlapping spheres: if spheres are drawn around the sites with a certain diameter, which are allowed to overlap, then the diameter, which leads to percolation, is just equal to r^* [2, 46].

Also the dynamics of the network for $s \neq 0$ has been demonstrated to be govened by the geometry and statistics of the continuum percolation cluster [43, 48–51].

6. Conclusions

We have demonstrated that the self-consistent ERM approximation [20] captures the salient features of the vibrational anomalies of disordered solids, namely Debye behavior and Rayleigh scattering at low frequency and an enhancement over the Debye law at higher frequencies (boson peak). At very high densities the spectrum is dominated by the 'liquid dispersion' $\omega(q) = \sqrt{(t_0 - t_q)}$ featuring a strong peak at the Einstein frequency t_0. This peak is broadened at lower densities as the influence of the frozen-in disorder takes over. At a critical density—within the self-consistent approximation—the spectrum becomes unstable, indicating the border of the validity of the SCERM and ERM-SCB approximations. It has been argued that the SCBA of heterogeneous-elasticity theory is based on Gaussian elasticity fluctuations, which, for a too broad distribution includes negative force constants. However, in real solids negative force constants exist, therefore the instability, which has been termed transition to a saddle phase [18] might exist in the trasformation towards the liquid state. The boson peak is then the precursor of this transition [13]. For the ERM model this transition does not occur.

The general dynamics of the ERM-type models changes smoothly with increasing Γ from the Einstein-type spectrum towards a spectrum dominated by the percolation cluster. Detailed model calculations by the present authors, covering this whole density range, are under way.

It is worth while to mention the power of the full vector ERM formalism based on equation (1). The formalism for this equation has been worked out by Ciliberti *et al* [19]. In spite of the mentioned shortcomings of the cactus approximation this work may serve as basis for further understanding the mixing of longitudinal and transverse high-frequency modes in liquids and disordered solids [65, 66].

ORCID iDs

Walter Schirmacher https://orcid.org/0000-0002-6301-8553
Carl Ganter https://orcid.org/0000-0002-6735-7448

References

[1] Mehta M L 1967 *Random Matrices* (New York: Academic)
[2] Efros A I and Shklovskiĭ B I 1984 *Electronic Properties of Doped Semiconductors* (Heidelberg: Springer)
[3] Brody T A, Flores J, French J B, Mello P A, Pandey A and Wong S S M 1981 *Rev. Mod. Phys.* **53** 385
[4] Wishart J 1928 *Biometrica* A **20** 32
[5] Wigner E P 1955 *Ann. Math.* **62** 548
[6] Beenakker C W J 1997 *Rev. Mod. Phys.* **69** 731

[7] Dyson F J 1962 *J. Math. Phys.* **3** 140
[8] Tulino A M and Verdú S 2004 *Random Matrix Theory and Wireless Communications* (Delft: Now Publishers)
[9] Hubbard J and Beeby J L 1969 *J. Phys. C: Solid State Phys.* **2** 556
[10] Xu B C and Stratt R M 1990 *J. Chem. Phys.* **92** 1923
[11] Wu T M and Loring R F 1990 *J. Chem. Phys.* **97** 8568
[12] Schirmacher W and Wagener M 1992 *Phil. Mag.* B **65** 861
[13] Schirmacher W, Diezemann G and Ganter C 1998 *Phys. Rev. Lett.* **81** 136
[14] Martín-Mayor V, Parisi G and Verroccio P 2000 *Phys. Rev.* E **62** 2373
[15] Grigera T S, Martín-Mayor V, Parisi G and Verrocchio P 2001 *Phys. Rev. Lett.* **87** 085502
[16] Martín-Mayor V, Mézard M, Parisi G and Verrocchio P 2001 *J. Chem. Phys.* **114** 8068
[17] Grigera T S, Martín-Mayor V, Parisi G and Verrocchio P 2001 *J. Phys.: Condens. Matter* **14** 2167
[18] Grigera T S, Martín-Mayor V, Parisi G and Verrocchio P 2003 *Nature* **422** 289
[19] Ciliberti S, Grigera T S, Martín-Mayor V, Parisi G and Verrocchio P 2003 *J. Chem. Phys.* **119** 8577
[20] Ganter C and Schirmacher W 2010 *Phys. Rev.* B **82** 094205
[21] Grigera T S, Martín-Mayor V, Parisi G, Urbani P and Verrocchio P 2011 *J. Stat. Mech.* P02015
[22] Folli V, Ruocco G and Schirmacher W 2017 *Frontiers Phys.* **5** 29
[23] Mézard M, Parisi G and Zee A 1999 *Nucl. Phys.* B **559** 689
[24] Elliott S R 1984 *The Physics of Amorphous Materials* (New York: Longman)
[25] Elliott S R 1992 *Europhys. Lett.* **19** 201
[26] Binder K and Kob W 2011 *Glassy Materials and Disordered Solids: an Introduction* (London: World Scientific)
[27] Schirmacher W 2015 *Theory of Liquids and Other Disordered Media* (*Lecture Notes in Physics* vol 887) (Heidelberg: Springer)
[28] Schirmacher W, Scopigno T and Ruocco G 2014 *J. Noncryst. Sol.* **407** 133
[29] Squires G L 1978 *Thermal Neutron Scattering* (Cambridge: Cambridge University Press)
[30] Shuker R and Gammon R W 1970 *Phys. Rev. Lett.* **25** 222
[31] Schmid B and Schirmacher W 2008 *Phys. Rev. Lett.* **100** 137402
[32] Monaco G and Giordano V M 2009 *Proc. Natl Acad. Sci. USA* **106** 3659
[33] Baldi G, Giordano V M and Monaco G 2011 *Phys. Rev.* B **83** 174203
[34] Rayleigh J W S L 1871 *Phil. Mag.* **41** 241
[35] Leonforte F L, Boissière R, Tanguy A, Wittmer J P and Barrat J L 2005 *Phys. Rev.* B **72** 224206
[36] Leonforte F L, Tanguy A, Wittmer J P and Barrat J L 2006 *Phys. Rev. Lett.* **97** 055501
[37] Monaco G and Mossa S 2009 *Proc. Natl Acad. Sci. USA* **106** 16907
[38] Marruzzo A, Schirmacher W, Fratalocchi A and Ruocco G 2013 *Sci. Rep.* **3** 1407
[39] Mizuno H, Mossa H and Barrat J L 2013 *Europhys. Lett.* **104** 56001
[40] Schirmacher W 2006 *Europhys. Lett.* **73** 892
[41] Schirmacher W, Ruocco G and Scopigno T 2007 *Phys. Rev. Lett.* **98** 025501
[42] John S, Sompolinky H and Stephen M J 1983 *Phys. Rev.* B **28** 5592
[43] Köhler S, Ruocco R and Schirmacher W 2013 *Phys. Rev.* B **88** 064203
[44] Akexander S, Bernasconi J, Schneider W R and Orbach R 1981 *Rev. Mod. Phys.* **53** 175
[45] Mott N F and Davis E A 1971 *Electronic Processes in Non-Crystalline Materials* (Oxford: Oxford University Press)
[46] Böttger H and Bryksin V V 1985 *Hopping Conduction in Solids* (Heidenheim: Verlag Chemie)
[47] Kirkpatrick S 1973 *Rev. Mod. Phys.* **45** 574
[48] Schrøder T B and Dyre J C 2000 *Phys. Rev. Lett.* **84** 310
[49] Schrøder T B and Dyre J C 2008 *Phys. Rev. Lett.* **101** 025901
[50] Amir A, Oreg Y and Imry Y 2010 *Phys. Rev. Lett.* **105** 070601
[51] Amir A, Krich J J, Vitelli V, Oreg Y and Imry Y 2013 *Phys. Rev.* X **3** 021017
[52] Ganter C and Schirmacher W 2011 *Phil. Mag.* **91** 1894
[53] Economou E N 1971 *Green's Function in Quantum Physics* (Heidelberg: Springer)
[54] Schirmacher W, Schmid B, Tomaras C, Viliani G, Baldi G and Ruocco G 2008 *Phys. Status Solidi* c **5** 862
[55] Varga R S 2010 *Gershgorin and His Circles* (Heidelberg: Springer)
[56] Marruzzo A, Köhler S, Fratalocchi A, Ruocco G and Schirmacher W 2013 *Eur. Phys. J. Spec. Top.* **216** 83
[57] Tomaras C and Schirmacher W 2013 *J. Phys.: Condens. Matter* **25** 495402
[58] Schirmacher W, Maurer E and Pöhlmann M 2004 *Phys. Status Solidi* c **1** 17

[59] Ferrante C, Pontecorvo E, Cerullo G, Chiasera A, Ruocco G, Schirmacher W and Scopigno T 2013 *Nat. Commun.* **4** 1793
[60] Ernst M H, Machta J, Dorfman J R and van Beijeren H 1984 *J. Stat. Phys.* **34** 477
[61] Hansen J and McDonald I 2006 *Theory of Simple Liquids* (Amsterdam: Elsevier)
[62] Machta J, Ernst M H and van Beijeren H 1984 *J. Stat. Phys.* **35** 413
[63] Höfling F, Franosch T and Frey E 2006 *Phys. Rev. Lett.* **98** 165901
[64] Gelin S, Tanaka H and Lemaître A 2016 *Nat. Mater.* **15** 1177
[65] Sampoli M, Ruocco G and Sette F 1997 *Phys. Rev. Lett.* **79** 1678
[66] Izzo M G, Wehinger B, Ruocco G, Matic A, Masciovecchio C, Gessini A and Cazzato S 2017 (arXiv:1705.10338)